Jurnal Teknologi

Full Paper

EFFECTIVENESS OF DIFFERENT DAMPING PAD GEOMETRIES IN REDUCING VIBRATION

Nazik Abdulwahid Jebur[a]*, Zahra Khalid Hamdan[a], Zaineb waired Metteb[a], Rafeaf. J. Salman[b]
[a]Mechanical Engineering Department, College of Engineering, Mustansiriyah University, Baghdad, Iraq
[b]Al-Musayyib Technical Institute, Al-Furat Al-Awsat Technical University, Iraq

Article history
Received
11 June 2024
Received in revised form
12 November 2024
Accepted
12 November 2024
Published Online
26 June 2025

*Corresponding author
nazikabdulwakid@uomustansiriyah.edu.iq

Graphical abstract

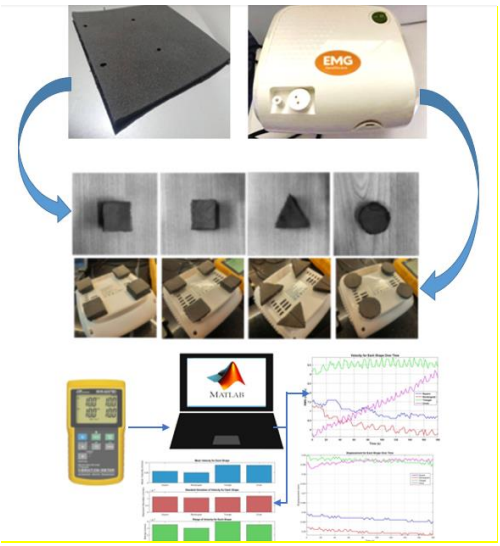

Abstract

This study aims to evaluate the effectiveness of different geometric shapes of damping pads in reducing vibrations, focusing on square, rectangular, triangular, and circular shapes. The pads were designed to have the same surface area, thickness, and materials to ensure a fair comparison. The main objective is to determine the most efficient shape for vibration reduction, especially in applications that require a quiet environment, such as vaporizer devices for asthma patients. Vibration velocity and displacement data were analyzed using MATLAB. The results showed that rectangular pads were the most effective, with a vibration velocity of 6.2 mm/s and a displacement of 0.0496 mm, achieving reduction percentages of 34.7% and 42.99%, respectively. The square shape demonstrated good stability with a vibration velocity of 7 mm/s and a displacement of 0.0565 mm, with reduction percentages of 26.3% and 35.2%. Triangular and circular pads were the least efficient in reducing vibrations. This study indicates that rectangular and square shapes are the most effective in reducing vibrations, making them suitable for applications that require a stable and quiet environment.

Keywords: Vibration Damping; Geometric Shapes; Damping Pads; Vibration Reduction; Vaporizer Devices

© 2025 Penerbit UTM Press. All rights reserved

1.0 INTRODUCTION

The summaries discuss many different techniques and methods for isolating and attenuating vibration [1]. The methods for isolating dynamic back-resonant vibration in rotorcraft, improving structural damping in high-speed lightweight trains with viscoelastic patches, optimizing the design of multi-mode shunt damping circuits with particle swarm optimization, and the performance of dynamic vibration absorbers based on elastomers are some of the topics covered in the abstracts [2,3]. Evolving techniques for adaptive magnetoelastic parameter optimization of fluid-elastic vibration isolators [4,5]. To better appreciate the background and necessity of improving the isolation efficacy of vibration-dampening pads, these summaries provide a detailed evaluation of the many methodologies utilized in the field of vibration isolation and damping [6, 7 ,8].

The benefits of vibration are little used from the effects of vibration and noise from various sources [9]. Different types of these pillows are designed for specific purposes [10]. Another type is universal vibration dampening and noise reduction material, which uses a flexible metal structure and organic

polymer material to dampen vibrations and reduce noise [11]. Cushions made from used car models have also been evaluated for their effectiveness in protecting buildings during earthquakes [4]. In addition, the vibration pad of the new mechanical equipment has been developed, incorporating compression springs and energy-reducing rubber blocks to effectively reduce severe vibrations [5]. New cohesion has also been worked on, using a multi-strength copolymer and strong efforts to achieve the durability of gold [8].

A dual-frequency vibration isolation system for helicopter reducers was the subject of the analysis and optimization design carried out by Liu *et al.* [1] (2023). In order to account for the vibrational properties of high-speed helicopters, they devised a system with two anti-resonant frequencies. In order to investigate how different parameters, affect vibration isolation performance, the study derived theoretical equations and determined the system's transmissibility. The theoretical results were confirmed to be accurate through model experiments. Initial optimization of the system's architecture was carried out using installation forms for helicopter reducers; this yielded useful information for the construction of vibration isolators for helicopters with varying speeds.

Marakakis *et al.* [3](2022) presented a new optimal design approach for multimode shunt-damping circuits to enhance vibration control. They modified the "current-flowing" shunt circuit to control multiple vibration modes of a piezoelectric laminate beam, considering resistor-damping components, capacitances, and shunting branch inductors as design variables. The study employed particle swarm optimization to minimize the H∞ norm of the damped system and conducted numerical models to compare the proposed method with others from the literature. Results demonstrated improved damping efficiency and reduced shunt inductance values, validating the effectiveness of the proposed design.

Melero *et al.* [4](2022) conducted an experimental analysis of constrained layer-damping structures for vibration isolation in lightweight railway vehicles. They aimed to maintain or increase structural stiffness and damping in lightweight train bodies. The study analyzed various design parameters' influence on damping performance, considering absolute and specific damping. Experimental results suggested that partial application of thin viscoelastic and constraining layers effectively increased structural damping without compromising weight, while full coverage with thick viscoelastic layers and honeycomb constraining layers yielded higher damping ratios.

Choi and Wereley [5](2022) evaluated the vibration isolation performance of an adaptive magnetorheological elastomer-based dynamic vibration absorber (MRE-DVA) for mitigating high-frequency vibrations of target devices. They designed a simple and effective MRE-DVA and experimentally measured its performance, observing a controllable dynamic stiffness range greater than two over the tested frequency range. Experimental results demonstrated improved vibration isolation performance using the adaptive MRE-DVA compared to traditional methods.

Chen [12] (2022) investigated the displacement transfer characteristic and parameter optimization design of a fluid-elastic isolator. They derived the equation of motion using the Lagrange principle and analyzed the effects of main design parameters on displacement transfer rate[13]. Parameter optimization was conducted using a genetic algorithm for civil helicopters, aiming to minimize displacement transfer rate while considering weight cost. Results showed that optimal parameters obtained by the genetic algorithm exhibited higher vibration isolation rates and lower weight costs compared to ordinary designs.

Peng *et al.* [14] (2022) conducted an experimental study on the vibration absorption performance of floating slabs of vibration isolation pads in metro shield tunnels., Jebur *et al.* [15] examined how different damping pads affected vibration dampening. And, their objective was to improve the vibration isolation efficiency via performing investigational researches upon the influences of various damping pad cross-sectional areas as well as thicknesses. The optimum design may be likely, as the outcomes elucidated that the amplitudes of vibration were considerably decreased with raising the goal of decreasing the buildings' seismic response of building.

Shirai and Park [16] (2020) evaluated the feasibility of employing STPs into a system of vibration control. For evaluating the capacity of damping and the mechanical properties of STP samples, they exposed them to the vertical loading and the dynamic loading tests. And, it was manifested that the STP samples actively decreased the seismic response if utilized in the structures, as proved via their steady hysteretic loops as well as the modest capability of damping. Also, a method to optimize the dampening pads distribution upon a body-in-white structure of car for reducing the structure-born noise was sugested via Sipos *et al.* [17] (2022). In addition, the layout of dampening pad was optimized employing vehicle acoustic simulation, causing a decrease of (33%) in the use of dampening pad with no compromising acoustic performance. Furthermore, a formulation of coupling agent, diene rubber, carbon black, and silica was presented by Nagata [18] (2018) anti-vibration rubber. Moreover, the mix aimed for rapid vulcanization with no lost of workability or durability. And, the investigation determined that the rubber having a carbon black-to-silica mix ratio possessed better anti-vibration characteristics as well as continued lengthier. The formulation of Nagata's anti-vibration rubber enhanced the durability and period of vulcanization.

He, Z. *et al.* [19] (2022) showed that the the Vibration Reduction and Frequency Modulation Device (VRFMD) effectiveness in improving the

performance of the damping of the Elastic Side-Supporting Long Sleeper Damping Track (ESSDT) depends greatly upon its geometrical characteristics. And, the VRFMD spring stiffness is vital in adjusting the natural frequency of the system, avoiding the wheel-rail resonance. The modifications in the design of device considerably decreased the vibrations and improved the stability of structure. Kraśkiewicz, C. *et al.* [20] (2023). The present study utilizes Artificial Neural Networks (ANNs) for predicting the bedding moduli of beneath Sleeper Pads (USPs) produced from the re-cycled rubber. Also, it show up the significance of geometrical characteristics, depicting that the augmented density enhances the isolation of vibration, whereas the thickness affects the performance. Models of ANN help design the maintainable USPs for the railway plans. Zhai, W. *et al.* [21] (2015) examined the ground vibrations reasoned via elevated-speed trains upon a non-ballasted track between Shanghai and Beijing. And, it showed up that the train geometrical arrangement, like the car spacing and wheelbase, considerably influences the features of vibration, like amplitude and frequency. And, the outcomes evinced that the speed of train and the geometrical design are critical parameters in handling the ecological vibrations.

Eventually, the present study discovers a diversity of methods and procedures for the vibration isolation and damping, concentration upon improving the dynamic dampers and vibration pads performance throughout the enhanced geometrical design as well as the progressed substances, like organic polymers and magnetorheological elastomers. This study aims to evaluate the effectiveness of different geometric shapes of damping pads in reducing vibrations and to identify the most efficient shape for applications that require a stable environment, such as vaporizer devices for asthma patients.

2.0 EXPERIMENTAL WORK

This section covers study details like materials and testing equipment. We will carefully test numerous dampening pads to determine which reduce vibration and noise best.

The next sections discuss the experimental setup, data gathering methods, and analysis methods used to evaluate each damping pad shape. The study examines these characteristics to find the best vibration mitigation methods for practical use.

2.1 Damping Pad

Dampers were initially constructed from a composite of natural and synthetic rubber, designed to optimize performance through the addition of several key materials. The mixture was enhanced with calcium carbonate, 1502 ground sponge material, zinc stearate, paraffin oil (also known as salamander oil), and carbon black, which is a silicon material. These components contributed to the pad's effectiveness in damping vibrations. The damping pad's core mechanical properties are summarized in Table 1, highlighting crucial attributes such as thickness, density, and tensile strength, as illustrated in Figure 1.

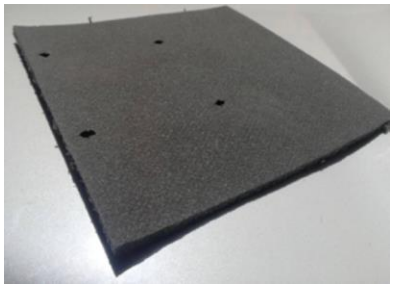

Figure 1 Damping pad

Table 1 Mechanical Properties of the Damping Pad [22-25]

Property	Description
Composition	Natural and synthetic rubber, carbon black, additives
Thickness	10 mm (1 cm)
Density	1.1 to 1.2 g/cm³
Hardness	50 to 70 Shore A
Tensile Strength	10-15 MPa
Elongation at Break	300-500%
Noise Reduction	Effective in minimizing noise levels
Durability	Resistant to UV light and moisture

2.2 Nebulizer

The nebulizer is a vital medical device designed to administer medication in the form of a fine mist that is directly inhaled into the lungs. This delivery method is particularly effective for treating a variety of conditions affecting both the upper and lower respiratory tracts, thereby enhancing the efficacy of respiratory therapy. The device's operational and performance characteristics are illustrated in Figure 2 and detailed in Table 2, which includes specifications such as input voltage, medication capacity, particle size distribution, and other relevant technical details.

Figure 2 Nebulizer

Table 2 Nebulizer Specifications

Specification	Details
Input Voltage	220V/50Hz
Power Consumption	180VA
Medication Capacity	6 ml
Particle Size (Respirable Fraction)	0.5 to 5 µm at 80%
Mass Median Aerodynamic Diameter (MMAD)	2.0 µm
Nebulization Rate	Above 0.2 ml/min
Operating Pressure Range	12-14.5 Psi (0.85-1.1 bar)
Airflow Rate	8-10 lpm
Noise Level	Below 60 dBA
Operating Temperature Range	10°C-40°C (50°F-104°F)
Operating Humidity Range	10% to 95% RH
Certifications	CE, ISO13485

The compressor component of the nebulizer is constructed from high-quality steel, designed to resist rust and maintain optimal functionality even during prolonged operation. Its design ensures efficient cooling, which contributes to its durability and performance. And, the compressor motor characteristically runs at an almost (3,000 RPM) speed, to ensure effective medication supply [26]. In addition, it's furnished with robust wiring for minimizing the noise, working at a (40 decibels) sound level or lower, as revealed in the Figure 3.

Figure 3 Compressor

2.3 Vibration Meters and Calibration

A vibration meter is a critical apparatus in the engineering and industrial uses, utilized for measuring the vibrations in articles as well as constructions through a broad range (10 Hz - 1 kHz) of frequency. And, the BVB-8207SD vibration meter, as displayed in the Figure 4, was utilized for collecting the data in the present work. Also, such apparatus highlights a big backlit LCD screen that evinces the readings from (4) channels concurrently and comprises (4) vibration sensors with magnetic attachments for securing the installation. In addition, the readings are saved upon an SD card in an Excel sheet format, enabling the easy transfer of data to a computer for the purpose of analysis.

One of the important benefits of the BVB-8207SD is its shortage of requisite for repeated re-calibration, chiefly owing to its supplementary VB-83 sensor module, which gets pre-calibrated with stowed calibration data. In accordance with the manual apparatus, such VB-83 sensor feature makes sure accurate readings wite no requisite for the re-calibration if substituting the sensor, thus saving the time and improving the efficacy as well as reliability in the long-lasting measurements [15].

Figure 4 BVB-8207SD Vibration Meter with VB-83 Sensor

2.4 Framework Components

In the context of the study investigating the efficacy of different damping pad shapes, the framework components encompass various elements crucial for conducting a systematic and comprehensive analysis. These components serve as the foundational structure guiding the experimental design, data collection, and interpretation of results.

2.4.1 Experimental Design

The framework includes the formulation of the experimental setup, encompassing the selection of damping pad shapes (square, rectangular, triangle, and circle) as independent variables.as shown in the Figure 5.

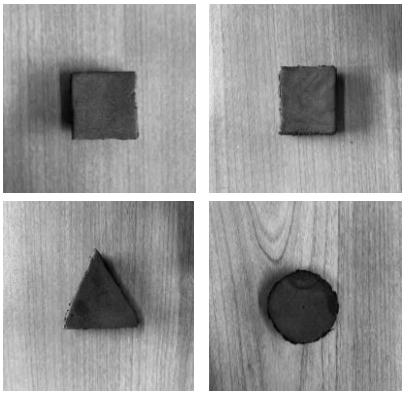

Figure 5 Damping pad shapes

It delineates the parameters held constant across all pads, such as surface area, thickness, and materials, ensuring a controlled environment for fair comparisons.

2.4.2 Data Collection Methodology

The framework outlines the methodology for collecting vibration velocity and displacement data using a vibration measuring device. It emphasizes the meticulous approach to data acquisition, ensuring accuracy and reliability in assessing the performance of each pad shape. The vibration sensor position is well located and installed as shown in the figure 6.

Figure 6 Vibration Sensor Positio

2.4.3 Geometric Properties of Damping Pads for Vibration Mitigation

A structured and description for each damping pad shape along with their dimensions and area Table 3. provides a concise and organized overview of the dimensions and areas for each damping pad shape:

Table 3 Specification of damping pad shape

Damping Pad Shape	Dimensions (Width x Length)	Area (cm^2)
Rectangular	2.6 cm x 3.5 cm	9
Square	3 cm x 3 cm	9
Triangular	Base: 5 cm, Height: 3.6 cm	9
Circular	Radius: 1.7 cm	9

These dimensions and areas are crucial for understanding the geometric properties of each damping pad shape and their potential impact on vibration and noise mitigation.

2.4.4 Placement of Damping Pads on the Device

A. A rectangular damping pad fitted under the device by removing the old base and setting it on top of the new one.
B: A square damping pad can be used in place of the original foundation in the same way as a rectangle pad.
C. Triangle Damping Pad: When used under the device's base, it functions similarly to the square and rectangular pads.
D. The circular damping pad is positioned beneath the device by removing the original base and replacing it with it, just like the other shapes (as illustrated in Figure 7.

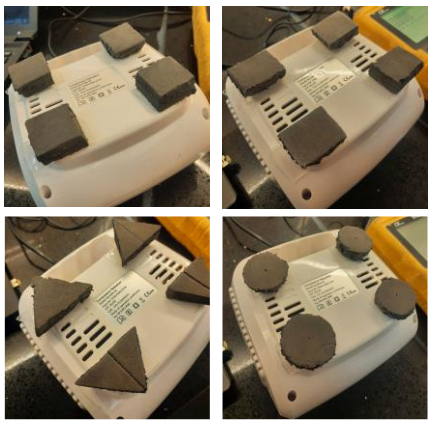

Figure 7 Placement of Damping Pads

3.0 RESULTS AND DISCUSSION

In this study, we explore the effectiveness of different damping pad shapes in reducing vibration. The experiment focused on four types of damping pads: square, rectangular, triangle, and circle. These pads were meticulously designed to have identical surface areas, thicknesses, and materials, ensuring a fair comparison.

Through testing using a vibration measuring device, we obtained valuable data on vibration velocity and displacement for each pad shape. Our ultimate goal is to identify the most efficient shape that minimizes vibration, particularly for applications where a tranquil environment is essential, such as vaporizer devices used by asthma patients and others.

In the subsequent analysis, we delve into the specific results obtained from each pad shape. By comparing the percentage decrease in vibration velocity and displacement, we aim to draw scientifically sound conclusions regarding the efficacy of each shape in vibration reduction. These findings are vital for improving performance and user comfort in a variety of applications by directing the selection of the ideal pad design.

3.1 Square Pad

The figures of velocity and displacement for the square pad show the steady motion during the observation time for (180 sec). And, the Root Mean Square (RMS) velocity starts at almost (7.5 mm/s), menifesting slight variations but in general reducing slowly to around (6.5 mm/s), showing an advanced slow down. In the meantime, the figure of

displacement demonstrates that the square's location stays steady, with minor oscillations within (0.055 mm) and (0.06 mm). Such observations elucidate the steadiness and trend of the square pad to keep balance, as verified via the Figures 8 and 9 for velocity and displacement, res[ectively.

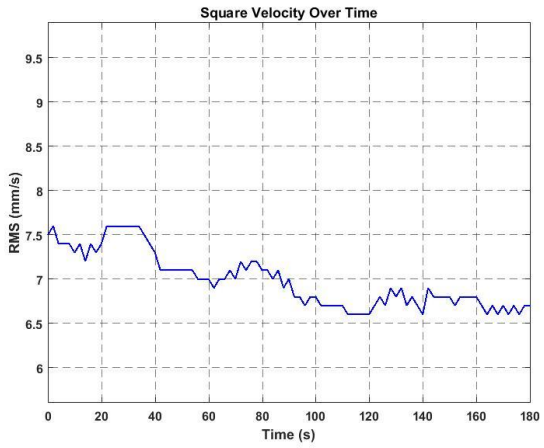

Figure 8 Time-Based Depiction of Vibration Velocity for Square Pad (RMS in mm/s during the Time in sec)

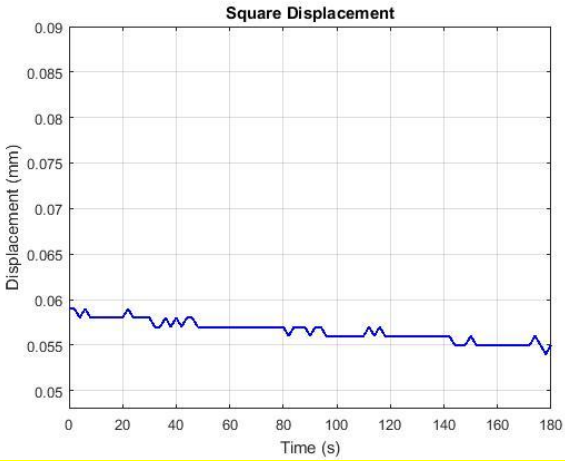

Figure 9 Time-Based Depiction of Vibration Displacement for Square Pad (Displacement in mm during the Time in sec)

3.2 Rectangular Pad

The figures 10 and 11 of the amalgamated analysis of velocity and displacement for the rectangle pad exhibits that the motion starts with an almost (7.5 mm/s) RMS velocity, which slowly reduces to around (6 mm/s) during a (180 sec) time. Such decrease in the velocity, in spite of slight fluctuations, portrays an overall tendency to slowing. Simultaneously, the displacement initiates at about (0.055 mm) and firstly displays minor oscillations prior to steadying at almost (0.05 mm). Such steadiness in the displacement reflects the trend of rectangle pad to keep its initial location during the time. Collected, such observations propose that the rectangle pad increasingly decelerates as well as steadies, emphasizing its capability for maintaining the steadiness and resisting the exterior disturbances.

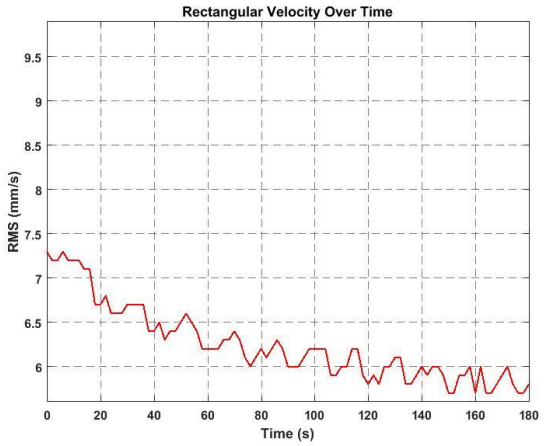

Figure 10 Time-Based Depiction of Vibration Velocity for Rectangular Pad (RMS in mm/s during the Time in sec)

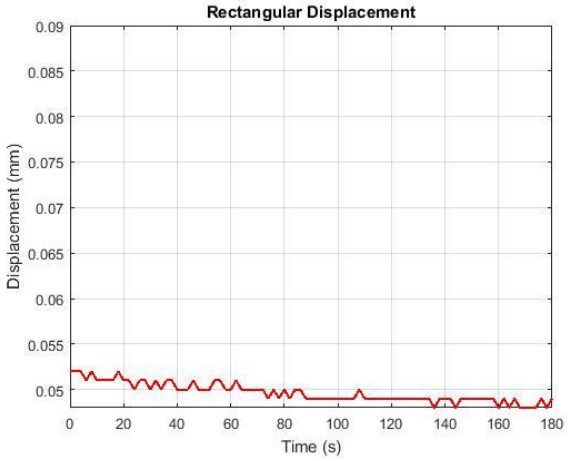

Figure 11 Time-Based Depiction of Vibration Displacement for Rectangular Pad (Displacement in mm during the Time in sec)

3.3 Triangle Pad

The Figures 12 and 13 of the amalgamated analysis of velocity and displacement for the rectangle pad exhibits that the motion starts with an almost (9 mm/s) average speed, showing important variations within (9 mm/s) and (9.5 mm/s) during the time of (180 sec). This suggests instability in the movement, with no clear trend towards deceleration or stabilization. Simultaneously, the displacement starts at around 0.085 mm and remains relatively stable, with slight oscillations around this value throughout the observation period. This indicates that while the triangle maintains its original position fairly well, it experiences small fluctuations in motion.

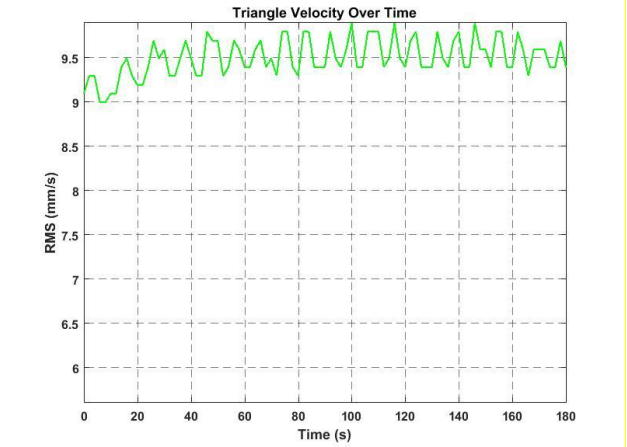

Figure 12 Time-Based Depiction of Vibration Velocity for Triangle Pad (RMS in mm/s during the Time in Sec)

Figure 13 Time-Based Depiction of Vibration Displacement for Triangle Pad (Displacement in mm during the Time in sec)

3.4 Circle Pad

The combined analysis of the velocity and displacement figures for the circle (Figures 14 and 15) shows that the velocity starts at approximately 6 mm/s and steadily increases to about 9.5 mm/s over 180 seconds, indicating constant acceleration. The displacement begins at around 0.085 mm and slightly increases to 0.09 mm, showing minor oscillations. These patterns suggest that the circle experiences continuous acceleration.

3.5 Comparison of Results Based on Percentage Reduction in Vibration Velocity and Displacement

The analysis of both vibration velocity and displacement data, as shown in Figures 16 and 17, reveals that the rectangular shape is the most effective in achieving stability. And, the rectangular shape depicts the ultimate percentage decreasing in the vibration velocity and displacement, exhibiting an elevated damping level and a sturdy capability for minimizing the deviation. And, this illustrates that the rectangle pad efficiently controls the positional motion as well as positional steadiness. Also, the square shape reveals a reduction in the velocity and displacement, displaying a certain steadiness degree, though it's less obvious than that for the rectangle shape.

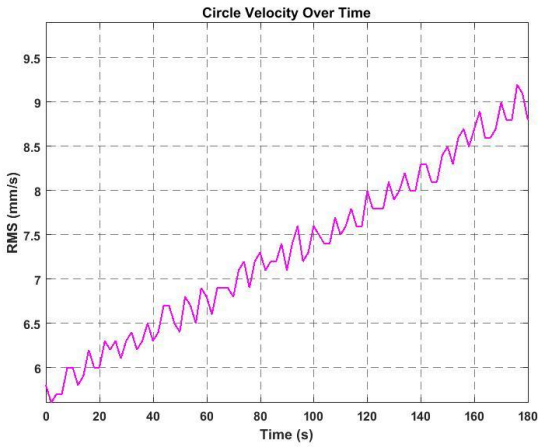

Figure 14 Time-Based Depiction of Vibration Velocity for Circle Pad (RMS in mm/s during the Time in Sec)

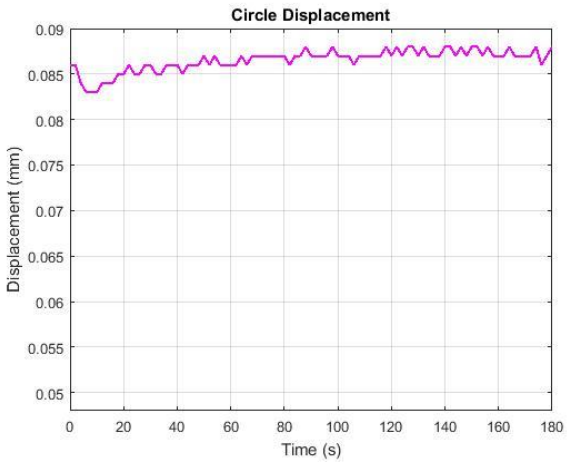

Figure 15 Time-Based Depiction of Vibration Displacement for Circle Pad (Displacement in mm during the Time in sec)

Additionally, in contrast, the triangle shape keeps an elevated and fixed speed with fixed displacement, and this reflects an instability as well as an oscillatory conduct with no important or decrease or damping. In the meantime, the circular shape manifests a rise in the speed and a minor rise in the displacement, depicting instability and acceleration, with a trend to diverge more from its initial location. Generally, the rectangular shape demonstrates to become the highly active at decreasing the vibration velocity and the vibration displacement, whereas the square shape is moderately active, and both the circle and triangle

shapes being less fruitful in preserving the steadiness beneath the prearranged circumstances.

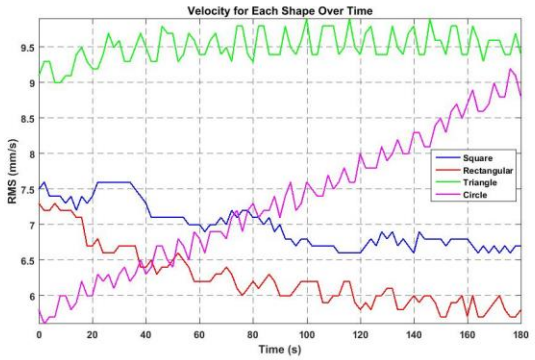

Figure 16 Time-Based Depiction of Vibration Velocity for (4) kinds of Pads (RMS in mm/s during the Time in sec)

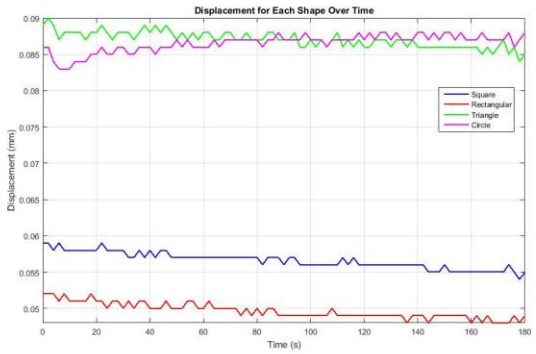

Figure 17 Time-Based Depiction of Vibration Displacement for (4) kinds of Pads (Displacement in mm during the Time in sec)

3.6 The Statistical Analysis of Dynamic Performance of the Geometrical Shapes

The statistical analysis takes a vital part in realizing the dynamic performance of different geometrical shapes, assisting to evaluate the steadiness of every shape as well as its capability for reducing the vibrations and deviations. Via employing statistical metric,s like mean, range, and standard deviation, it's likely to classify the highly active shapes in keeping steadiness across various engineering uses. Such analysis is vital to optimize the design and ensure the optimum performance in the surroundings that need minimum oscillation and undesirable movement. And, the statistical data listed in the Table 4 give a complete overview of the various geometrical shapes performance with respect to the displacement.

Table 4 The displacement's statistical measurements for different geometrical shapes

Shape	Mean Displacement (mm)	Standard Deviation of Displacement (mm)	Range of Displacement (mm)
Square	0.056593	0.0011351	0.005
Rectangular	0.049648	0.001058	0.004
Triangle	0.087044	0.0010946	0.006
Circle	0.086538	0.0011954	0.005

And, the statistical outcomes in the Table 1 reveals that the rectangular shape are the highly active in accomplishing the dynamic steadiness. Additionally, the rectangle shape possesses the lowermost mean displacement (0.049648 mm), the minimum displacement range (0.004 mm), and the lowermost standard deviation (0.001058 mm), depicting its elevated capability for maintaining its location and minimizing the deviations.

Also, in contrast, the square shape elucidates merely a minor decrease in the velocity as well as the displacement, showing the moderate steadiness in comparison with the rectangle shape. In addition, the triangle keeps the fixed velocity and displacement, and this reflects a shortage of an important enhancement in the steadiness or the deviations decrease. In the meantime, the circular shape portrays a rise in the speed as well as a minor rise the in displacement, depicting the acceleration and the deviation from the initial location, creating it the minimum steady among the investigated shapes.

Figures 18 and 19 display the dynamic performance ofthe various shapes, where the Figure 18 shows the comparison in the vibration velocity, and Figure 19 presents the comparisons in the displacement.

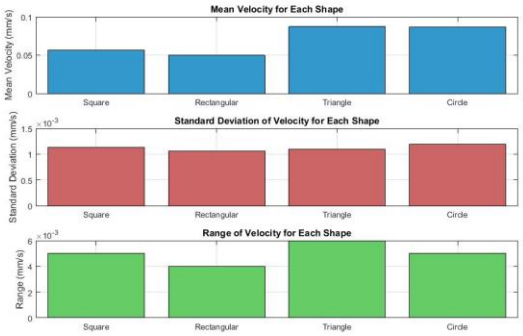

Figure 18 Statistical Characteristics of Displacement for Each Shape

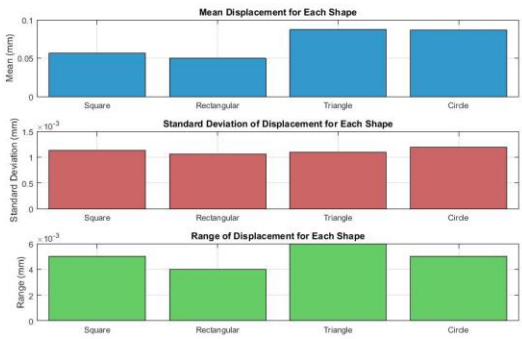

Figure 19 Statistical Characteristics of Velocity for Each Shape

4.0 CONCLUSION

The aim of the current study is to assess the efficiency of various geometrical shapes of damping pads in decreasing vibrations. And, the experimentation concentrated upon (4) kinds of pads: Square, rectangular, triangular, and circular. Such pads were designed to possess same materials, thickness, and surface areas for ensuring a reasonable comparison among the various shapes. Also, the main goal of the present study is to obtain the highly effective shape to minimize the vibrations, which being vital for the uses that need a calm atmosphere, like the vaporizer apparatuses employed via the asthma patients.

Analysis of the data of vibration velocity and displacement was carried out employing MATLAB (Version R2015b), which is a software tool broadly utilized for the mathematical as well as the statistical analysis, in addition to the data visualization. And, the outcomes manifested that the rectangular shape was the highly active in accomplishing the steadiness, as when the hieghest decrease in the vibration velocity and displacement was registered. Also, this reflects an elevated damping level and a capability for reducing the deviations and control the motion effectually.

The statistical measures, like mean, range, and standard deviation were computed employing MATLAB for assessing the steadiness of each shape. And, the rectangle shape possesses the lowermost mean displacement (0.049648 mm), the minimum displacement range (0.004 mm), and the lowermost standard deviation (0.001058 mm), verifying its elevated capability for maintaining the location and minimizing the deviations.

Additionally, in contrast, the square shape portrayed the moderate steadiness, with a (0.056593 mm) mean displacement. And, the triangular shape didn't demonstrate important enhancement in the steadiness, with a (0.087044 mm) mean displacement. Also, the circular shape was the minimum stable, depicting the acceleration as well as the deviation from its initial location, with a (0.086538 mm) mean displacement.

In general, the rectangular shape evidenced to become the highly active in decreasing the vibration velocity as well as the displacement, pursued via the square shape, which provides the moderate efficiency. And, the circular and triangular shapes being less fruitful in keeping the steadiness beneath the prearranged circumstances, where the circular shape was the minimum steady. Also, the present study gives valued visions to improve the damping pads design in the uses that need reducing the oscillation and the undesirable movement. Additionally, Table 5 depicts the comparative assessment of Vibration-Reduction damping pad shapes, indicating the percentage reduction in vibration velocity (PRV) as well as the percentage reduction in displacement (PRD).

Table 5 Comparative Assessment of the Vibration-Reduction Damping Pad Shapes

Pad Shape	Vibration Velocity (mm/s)	PRV%	Vibration Displacement (mm)	PRD%
Square	7	26.3	0.0565	35.2
Rectangular	6.2	34.7	0.0496	42.99
Triangle	9.5	-	0.087	-
Circle	7.3	23.2	0.0865	0.6

Acknowledgement

The authors thankfully acknowledge the Universty of A-Mustansiriyah (www.uomustansiriyah.edu.iq) for utilizing the facilities in the Labs of Mechanical Engineering Department/College of Engineering.

Conflicts of Interest

The author(s) declare(s) that there is no conflict of interest regarding the publication of this paper.

References

[1] Liu, C., Feng, Z., Xing, L., Yuan, X., & Dai, Z. 2023. Research and Optimization Design of Dual-frequency Vibration Isolation System for Helicopter Reducer. *Journal of Physics: Conference Series*. 2510(1): 012012. Doi: 10.1088/1742-6596/2510/1/0120.

[2] Dunbabin, M., Brosnan, S., Roberts, J., & Corke, P. 2004. Vibration Isolation for Autonomous Helicopter Flight. *IEEE International Conference on Robotics and Automation, 2004. Proceedings.* ICRA'04. 4: 3609-3615. Doi: https://doi.org/10.1109/ROBOT.2004.1308812.

[3] Marakakis, K., Tairidis, G. K., Foutsitzi, G. A., Antoniadis, N. A., & Stavroulakis, G. E. 2022. New Optimal Design of

Multimode Shunt-Damping Circuits for Enhanced Vibration Control. *Signals.* 3(4): 830–856. Doi: https://doi.org/10.3390/signals3040050.

[4] Melero, M., Nieto, A. J., Morales, A. L., Palomares, E., Chicharro, J. M., Ramiro, C., & Pintado, P. 2022. Experimental Analysis of Constrained Layer Damping Structures for Vibration Isolation in Lightweight Railway Vehicles. *Applied Sciences*. 12(16): 8220. Doi: https://doi.org/10.3390/app12168220.

[5] Choi, Y., & Wereley, N. M. 2022. Vibration Isolation Performance of an Adaptive Magnetorheological Elastomer-based Dynamic Vibration Absorber. *Actuators.* 11(6): 157. Doi: https://doi.org/10.3390/act11060157.

[6] R. A. Ibrahim. 2008. Recent Advances in Nonlinear Passive Vibration Isolators. 314(3–5): 371–452. Doi: http://doi: 10.1016/j.jsv.2008.01.014.

[7] Lu, Ze-Qi; Chen, Li-Qun; Brennan, Michael J.; Li, Jue-Ming; Ding, Hu. 2016. The Characteristics of Vibration Isolation System with Damping and Stiffness Geometrically Nonlinear. *Journal of Physics: Conference Series*. 744(): 012115. Doi: Http:// Doi:10.1088/1742-6596/744/1/012115.

[8] Negmatov, S., Ulmasov, T., Navruzov, F., & Jovliyev, S. 2021. Vibration Damping Composition Polymer Materials and Coatings for Engineering Purpose. E3S Web of Conferences. 264: 05034. Doi: http://dx.doi.org/10.1051/e3sconf/202126405034.

[9] Ljungberg, J. K., Parmentier, F. B. R. 2010. Psychological Effects of Combined Noise and Whole-body Vibration: A Review and Avenues for Future Research. *Proceedings of the Institution of Mechanical Engineers, Part D: Journal of Automobile Engineering*. 224(10): 1289–1302. Doi: http:// doi:10.1243/09544070JAUTO1315.

[10] C. H. Lee, M. Kawatani, C. W. Kim, N. Nishimura, Y. Kobayashi. 2006. Dynamic Response of a Monorail Steel Bridge under a Moving Train. 294(3): 562–579. Doi: http:// doi:10.1016/j.jsv.2005.12.028.

[11] R Lewandowski and B Chorazyczewski. 2010. Identification of the Parameters of the Kelvin–Voigt and the Maxwell Fractional Models, Used to Modeling of Viscoelastic Dampers. *Computers & Structures*. 88: 1–17. Doi: https://doi.org/10.1016/j.compstruc.2009.09.001.

[12] Chen, C. H. 2022. Investigation of the Displacement Transfer Characteristic and Parameter Optimization Design of Fluid-Elastic Isolator. Doi: 10.3233/ATDE221096.

[13] Shin, Y. H., Kim, D., Son, S., Ham, J. W., & Oh, K. Y. 2021. Vibration Isolation of a Surveillance System Equipped in a Drone with Mode Decoupling. *Applied Sciences*. 11(4): 1961. Doi: http:// doi.org/10.3390/app11041961.

[14] Peng, G., Fu, K., Zhang, F., Bai, J., Zeng, Z., Li, Z., ... & Tang, Q. 2022. Experimental Study on Vibration Absorption Performance of Floating Slabs of Vibration Isolation Pads in Metro Shield Tunnels. Journal of Physics: Conference Series. 2185(1): 012061 Doi: 10.1088/1742-6596/2185/1/012061.

[15] Jebur, N. A., Ali, H. A. K., Abdulrazzaq, M. A., Abdulla, F. A., & Hamdan, Z. K. 2023. Investigation Of Various Damping Pads Effect on Vibration. AIP Conference Proceedings. 2787(1). Doi: https://doi.org/10.1063/5.0148204.

[16] Shirai, K., & Park, J. 2020. Use of Scrap Tire Pads in Vibration Control System for Seismic Response Reduction of Buildings. *Bulletin of Earthquake Engineering*. 18(5): 2497–2521. Doi: https://doi.org/10.1002/stc.2324.

[17] Sipos, D., Treszkai, M. F., & Feszty, D. 2022. Optimization of Damping Pad Distribution on Body-in-white Car Structure. *Journal of Vibroengineering*. 24(2): 386–393. Doi: https://doi.org/10.21595/jve.2021.22158.

[18] Nagata, T. 2018. U.S. Patent Application No. 15/736,641. Doi: https://zenodo.org/doi/10.5281/zenodo.11220536.

[19] He, Z., Zhai, W., Wang, Y., Shi, G., Bao, N., Yuan, X., ... & Wang, H. 2022. Theoretical and Experimental Study on Vibration Reduction and Frequency Tuning of a New Damped-Sleeper Track. *Construction and Building Materials.* 336: 127420. Doi: https://doi.org/10.1016/j.conbuildmat.2022.127420.

[20] Kraśkiewicz, C., Anysz, H., Zbiciak, A., Płudowska-Zagrajek, M., & Al Sabouni-Zawadzka, A. 2023. Artificial Neural Networks as a Tool for Selecting the Parameters of Prototypical Under Sleeper Pads Produced from Recycled Rubber Granulate. *Journal of Cleaner Production.* 405: 136975. Doi: https://doi.org/10.1016/j.jclepro.2023.136975.

[21] Zhai, W., Wei, K., Song, X., & Shao, M. 2015. Experimental Investigation into Ground Vibrations Induced by Very High Speed Trains on a Non-ballasted Track. *Soil Dynamics and Earthquake Engineering*. 72: 24–36 Doi: https://doi.org/10.1016/j.soildyn.2015.02.002.

[22] Mark, E. J., Erman, B., & Eirich, F. R. 2005. *The Science and Technology of Rubber.* Elsevier Academic Press.

[23] Donnet, J. B. (Ed.). 2018. *Carbon Black: Science and Technology*. Routledge.

[24] Pospisil, J., & Nespùrek, S. 2000. 3 Additives for plastics and their transformation products (pp. 47-48). Plastic packaging materials for food: barrier function, mass transport, quality assurance, and legislation.

[25] Franta, I. (Ed.). 2012. Elastomers and Rubber Compounding Materials (Vol. 1). Elsevier.

[26] https://sunsethcs.com/product/neb100-compressor-nebulizer/